Optics Letters

Compact all-fiber light-induced thermoelastic spectroscopy for gas sensing

Lien Hu,[1] Chuantao Zheng,[1,*] Yu Zhang,[1] Jie Zheng,[1] Yiding Wang,[1] and Frank K. Tittel[2]

[1]State Key Laboratory of Integrated Optoelectronics, College of Electronic Science and Engineering, Jilin University, Changchun 130012, China
[2]Department of Electrical and Computer Engineering, Rice University, Houston, Texas 77005, USA
*Corresponding author: zhengchuantao@jlu.edu.cn

Received 22 January 2020; revised 26 February 2020; accepted 26 February 2020; posted 28 February 2020 (Doc. ID 388754); published 20 March 2020

To overcome the limitations of size, optical alignment, and integration into photonic circuits in previous light-induced thermoelastic spectroscopy (LITES) using free-space optics, a compact all-fiber LITES was proposed for gas sensing. A hollow-core photonic crystal fiber was employed as a waveguide and a microcapillary gas cell simultaneously. A single-mode fiber (SMF) tip was employed to guide light on the quartz tuning fork (QTF) surface. The distance between the SMF tip and the QTF, and the light excitation position on the QTF's surface were optimized experimentally. The detection performance of the all-fiber LITES was evaluated by detecting methane, and a normalized noise equivalent absorption coefficient of 9.66×10^{-9} cm$^{-1} \cdot$ W Hz$^{-1/2}$ was realized at a 1 atm pressure and an environmental temperature of ∼297 K. The combination of fiber sensing and LITES allows a class of LITES sensors with compact size and potential for long-distance and multi-point sensing.

https://doi.org/10.1364/OL.388754

Laser absorption spectroscopy, which relies on the "finger-print" absorption lines of molecules for identifying and detecting trace chemicals, is a powerful technique that offers high selectivity and sensitivity [1,2]. A quartz tuning fork (QTF) has been used in laser absorption spectroscopy gas sensors since 2002 and has resulted in a wide range of applications in recent years due to low cost, small size, and a high quality-factor (Q-factor) of the QTF [3,4]. The first proposed gas detection scheme based on the QTF was named as quartz-enhanced photoacoustic spectroscopy (QEPAS) [3], which uses a QTF instead of a microphone as a sharply resonant acoustic transducer and improves the immunity of photoacoustic spectroscopy to environmental acoustic noise due to a high Q-factor of the QTF. However, the QEPAS sensor needs a resonance tube to achieve a resonance enhancement of the photoacoustic signal and a careful assembly and alignment process to achieve strong acoustic coupling and a high detection sensitivity without noise caused by light radiation [5–8]. Furthermore, the QTF must be immersed in the sample gas in QEPAS, which limits the application of this technique in long-distance and stand-off sensing.

Recently, the QTF was used as a thermoelastic transducer, which transforms the photothermal energy generated by light absorption into a mechanical motion and further converts it into an electrical signal utilizing the piezoelectric effect of quartz. This spectroscopic technique was first reported in 2018 and was named light-induced thermoelastic spectroscopy (LITES) or quartz-enhanced photothermal spectroscopy [9]. The gas sensor based on LITES without the need of a resonance tube shows an excellent detection performance compared to a QEPAS-based gas sensor and has attracted the attention of researchers [4,9–12]. However, until now, all LITES gas sensing systems are based on free-space optics [4,9,12] which to some degree limits the size of the sensor system, the conciseness of optical alignment, and the possibility of integration into the photonic circuits.

In this Letter, a compact all-fiber LITES was proposed to overcome the limitations of size, optical alignment, and integration into photonic circuits in free-space LITES. A hollow-core photonic crystal fiber (HC-PCF), which confines the gas sample and propagating light modes simultaneously within the hollow core, instead of a multi-pass cell (MPC), was employed to reduce the size of the sensor system. In addition, the light signal with absorption that excites the QTF mechanical vibration was guided on the QTF surface by a single-mode optical fiber (SMF) tip rather than an optical lens, which realizes a small size, low-cost, and easy light alignment process simultaneously. Furthermore, the all-fiber design makes it possible for LITES sensors to be integrated into the photonic circuits. Combined with a proper design [13], the all-fiber LITES will be useful for long-distance and multi-point sensing due to the low transmission loss of the employed all-fiber components.

An all-fiber LITES sensor system was realized as illustrated in Fig. 1. A distributed feedback (DFB) diode laser was used as the excitation source to target the R-branch $R(3)$ of the $2\upsilon_3$-band of methane (CH_4) at 6046.95 cm^{-1} with a line intensity of 1.45×10^{-21} cm^{-1}/(mol $\cdot$ cm^{-2}). The laser temperature was controlled at 27°C by a temperature controller (Thorlabs, Model TED 200C), and the driver current was modulated by a current driver (Thorlabs, Model LDC202C) with a composite

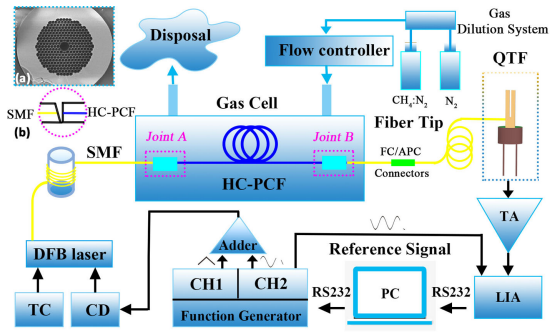

Fig. 1. Experimental setup. TC, temperature controller; CD, current driver; DFB laser, distributed feedback diode laser; SMF, single-mode fiber; HC-PCF, hollow-core photonic crystal fiber; QTF, quartz tuning fork; TA, trans-impedance amplifier; LIA, lock-in amplifier.

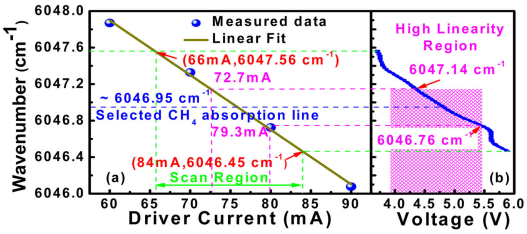

Fig. 2. (a) Wavenumber of the DFB laser as a function of the driver current, where the measured data were obtained by a Fourier transform spectrometer (Thermo Fisher Scientific, Model Nicolet iS50) and (b) the output voltage of the PD as a function of the laser wavenumber.

signal including a sine wave and a triangular wave generated by a function generator (Good Will Instrument, Model AFG-2225), where the modulation depth was set to 0.18 cm^{-1}. A QTF (KDS, Model DT-38) was used as a thermoelastic transducer. The resonant frequency f, Q-factor, and equivalent electrical resistance R were measured to be 32762.29 Hz, and 10476 and 135.14 kΩ, respectively, at 1 atm pressure and an environmental temperature of ∼297 K. The output light of the laser was launched into a SMF (Corning, Model SMF-28), which was butt-coupled to a ∼30 cm long HC-PCF (NKT Photonics, Model HC-1550-02) by two ceramic ferrules and a ceramic mating sleeve. A scanning electron microscope (SEM) image of the HC-PCF is shown in the inset (a) of Fig. 1. To avoid Fresnel reflections, the SMF was angle cleaved, leaving a gap to allow the gas access in the HC-PCF [see the inset (b) of Fig. 1]. The other end of the HC-PCF was spliced to another SMF in the same way. Finally, the light signal with absorption from the SMF was guided to the QTF surface by a SMF tip. The current generated by the QTF was converted to a voltage by a trans-impedance amplifier with a 10 MΩ feedback resistor. With an integration time of 0.3 s, the voltage was demodulated at the resonant frequency f of the QTF by a lock-in amplifier (Stanford Research System, Model SR830) to evaluate the detection performance of the all-fiber LITES sensor system.

The performance of the laser absorption spectroscopic gas sensors using a HC-PCF as a waveguide and a gas cell are usually limited by mode interference [14,15]. A suitable distance between the input SMF and the HC-PCF reduces the mode interference noise [15]. To minimize the effect of mode interference, the input SMF was adjusted for optimizing the coupling between the input SMF and the HC-PCF while linearly scanning the laser current (66–84 mA) for changing the emission wavenumber (6047.56 − 6046.45 cm^{-1}), as shown in Fig. 2(a). This adjustment process can be divided into two steps: (1) the distances between the SMF and the HC-PCF at the joints A and B were reduced as much as possible in order to realize a high coupling efficiency between the SMF and the HC-PCF; (2) the distance between the input SMF and the HC-PCF at joint A was further adjusted slightly by bending the input SMF to minimize mode interference. After the fine adjustment, the HC-PCF and the SMF were firmly fixed with the connectors by epoxy resin glue for enhancing the connection strength. The output optical power from the output SMF tip should be increased with the current linearly when no interference occurs. A photoelectric detector (PD) was employed to observe the optical power fluctuations from the output SMF tip. As shown in Fig. 2(b), an obvious nonlinearity of the output voltage of the PD, which is linearly related to the optical power, was observed due to the influence of multimode interference. However, a high linearity region was obtained by means of a fine adjustment. In order to reduce the effect of mode interference, the driver current range was set to be 72.7–79.3 mA, which extracts the second harmonic signal (2f-signal), while the selected CH_4 absorption line is located at 6046.95 cm^{-1}, and the reduced wavenumber range (6046.76 to 6047.14 cm^{-1}) is ∼2.5 times that of the full width half-maximum of the selected CH_4 absorption line (∼0.15 cm^{-1}). The output optical power of the SMF tip was ∼300 μW with a ∼7 mW power of the laser at the CH_4 absorption line (∼6046.95 cm^{-1}) due to a ∼12 dB coupling loss between SMFs and the HC-PCF.

The theoretically optimal optical excitation position on the QTF surface was the bottom of the QTF's prongs [4]. Therefore, we first investigated the effect on the 2f-signal amplitude of the distance Z between the SMF tip and the QTF [shown in the inset (i) in Fig. 3(b)] by adjusting the SMF tip to guide light at the bottom of the QTF's prongs. The HC-PCF was placed in a gas cell with a volume of 25 × 8 × 4 cm^3. A calibrated standard CH_4:N_2 mixture with a concentration level of 5000 parts per million by volume (ppmv) was pressurized into the gas cell at a flow rate of 300 standard cubic centimeter per minute (sccm). The optimization was carried out after the gas sample was completely immersed in the ∼30 cm long HC-PCF through free diffusion, which takes ∼1 h and can be judged by the fact that the amplitude of the 2f-signal reaches a stable value [14]. The 2f-signal amplitude as a function of the distance Z is plotted in Fig. 3(b). The electric field distribution of the SMF tip can be described by a Gaussian profile, and the waist radius w of the output beam increases with the distance Z ($w = w_0 \cdot (1 + (\lambda \cdot Z/(\pi \cdot w_0^2))^2)^{1/2}$, where w_0, ∼5 μm is the mode field radius of the SMF, and λ is the wavelength, i.e., 1.65 μm) at the QTF surface. The reflectivity of the QTF surface without silver film is lower than that with a silver film and provides a condition conducive to photon absorption. Therefore, the amplitude of the 2f-signal decreases with the increase of distance Z due to a reduced power density on the optimal excitation position at the bottom of the QTF's prongs without a silver film, as shown in the inset (ii) in Fig. 3(b). In order to improve the detection performance of the all-fiber LITES sensor, the SMF tip should be as close to the QTF surface as possible to obtain a smaller beam waist radius and less laser radiation loss in the air.

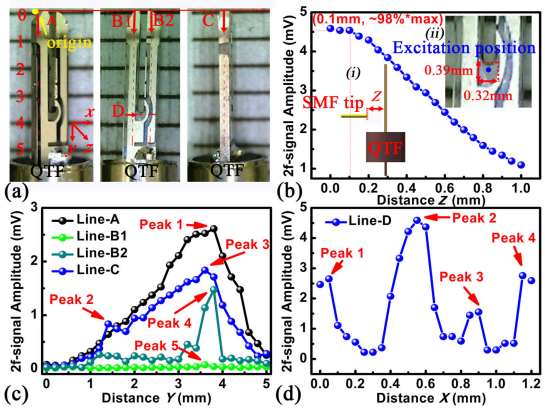

Fig. 3. (a) Schematic diagram of the beam excitation position optimization; (b) the 2 f-signal amplitude as a function of the distance Z [as shown in the inset (i)], where the excitation position was shown in the inset (ii); (c) the distance Y; and (d) the distance X. Line A, laser guided on the front edge of the QTF's prong; Line B1, laser guided on the front center of the QTF's left prong; Line B2, laser guided on the front center of the QTF's right prong; Line C, laser guided on the side of the QTF's prong. The origin of the coordinates (yellow point) is in the upper left corner of the front surface of the QTF.

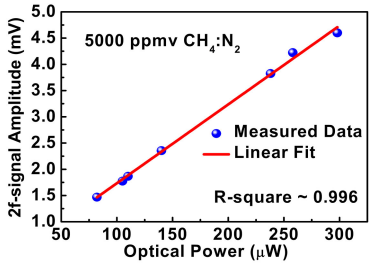

Fig. 4. 2 f-signal amplitude as a function of the output light power of the SMF tip, where the CH_4 concentration was 5000 ppmv.

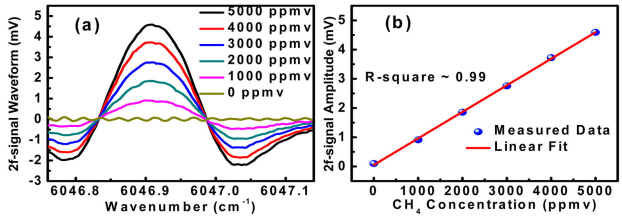

Fig. 5. (a) 2 f-signal waveform and (b) the 2 f-signal amplitude for CH_4:N_2 mixtures with six different concentration levels.

The laser beam excitation position employed in the all-fiber LITES was also optimized carefully for five different paths [Lines A, B1, B2, C, and D, as shown in Fig. 3(a)]. The corresponding optimized results are plotted in Figs. 3(c) and 3(d). To avoid damaging the SMF tip during the position adjustment process, the distance Z between the SMF tip and the QTF surface was set to 0.1 mm. The selection of this value is because the 2 f-signal amplitude is not significantly reduced at this distance, as shown in Fig. 3(b). The experimental results for Lines A, B1, and C are similar to the optimization results proposed in a free-space LITES sensor system [9]. A more detailed investigation for Lines B2 and D was carried out for the proposed all-fiber LITES. The piezoelectric signal generated by the QTF is related to the deformation of the QTF prongs, the QTF prong is bent to an angle with a certain degree at the excitation position, and the deviation of the QTF tip is directly proportional to the distance between the tip and that position as claimed in Ref. 9. This can be an explanation for why the 2 f-signal amplitude increases with the increase of distance Y for Lines A, B1, B2, and C, and the emergence of peaks 1, 3, 4, and 5 with a $Y \sim 3.9$ mm at the bottom of the QTF's prongs, as shown in Fig. 3(c). A Y-value > 3.9 mm leads to a reduced 2 f-signal amplitude due to an increased thermal diffusion area and a larger transmission loss. The emergence of peak 2 and a more sudden increase of peak 4 compared to that of peak 5 reveals that a QTF surface without silver film is more conducive to photon absorption. The 2 f-signal amplitude for Line A is higher than that for Lines B1, B2, and C due to a reduced silver film region, too. Although a similar silver film coverage was observed for Lines B1 and Line C, a higher 2 f-signal amplitude was obtained for Line C. This is because an excitation position on the side of the QTF's prong is more suitable to excite the QTF vibration at the fundamental flexural mode due to the same direction for the laser beam propagation and the QTF prong vibration. We further optimized the distance X with the optimized distance Y (~3.9 mm). Four peaks corresponding to four regions without silver film coverage for Line D [shown in Fig. 3(a)] were observed during the measurement as plotted in Fig. 3(d). An optimal position at the middle of the QTF's prong bottom was obtained. The optimal excitation position ($X \sim 0.55$ mm, $Y \sim 3.9$ mm, $Z = 0$ mm) for the proposed all-fiber LITES was employed to realize an optimal detection performance in the subsequent experiments.

To verify the linearity of the all-fiber LITES signal for the output power, an adjustable optical attenuator was connected in series between the output SMF and the SMF with a SMF tip. As shown in Fig. 4, the 2 f-signal amplitudes for seven different output light powers from ~80 to ~300 μW were recorded, and the linear fitting with an R-square value of ~0.996 reveals that the 2 f-signal amplitude establishes a highly linear response with the laser power.

Several calibrated standard CH_4:N_2 mixtures with concentration levels of 0, 1000, 2000, 3000, 4000, and 5000 ppmv were prepared by a gas dilution system (Environics, Model S4000) and pressurized into the gas cell at a flow rate of 300 sccm. For each concentration level, the demodulated 2 f-signal waveform was recorded after the gas was completely immersed in the HC-PCF. The measured 2 f-signal waveforms for different concentration levels were plotted in Fig. 5(a), and the corresponding 2 f-signal amplitudes were recorded in Fig. 5(b). An obvious asymmetry for the 2 f-signal waveform was observed due to the simultaneous change of laser power and wavelength by adjusting the laser current [16]. The linearity fitting results for the 2 f-signal amplitude and CH_4 concentration were also given in Fig. 5(b). The calculated R^2 value of ~0.99 shows that the demodulated 2 f-signal amplitude has an excellent linear response to the CH_4 concentration in the range of 0–5000 ppmv for the all-fiber LITES sensor.

The minimum detection limit of the all-fiber LITES sensor was investigated by a signal-to-noise ratio evaluation. The measured 2 f-signal waveform for 5000 ppmv CH_4:N_2 was plotted in Fig. 6(a). The noise was evaluated with pure N_2, as shown in Fig. 6(b). The 2 f-signal amplitude for 5000 ppmv CH_4:N_2 is

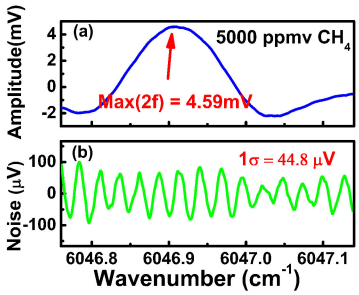

Fig. 6. (a) 2 f-signal waveform for a 5000 ppmv CH_4:N_2 mixture and (b) the background noise obtained with pure N_2.

Table 1. Detailed Comparison Between the Free-Space LITES and the Proposed All-Fiber LITES[a,b]

Method	Detection unit	Absorption line (cm^{-1})	Noise	NNEA ($cm^{-1} \cdot W \cdot Hz^{-1/2}$)
Free-space LITES[4]	Standard QTF	4291.50 (CO)	4.2 μV at 60 ms[b]	7.4×10^{-10}
Free-space LITES[9]	Standard QTF	6534.37 (C_2H_2)	4.22 μV at 1 s	7.63×10^{-9}
Free-space LITES[12]	Custom QTF	6534.37 (C_2H_2)	3.5 μV at 1 s	9.16×10^{-10}
All-fiber LITES[this]	Standard QTF	6046.95 (CH_4)	44.8 μV at 0.3 s	9.66×10^{-9}

[a]LITES, light-induced thermoelastic spectroscopy; MPC, multi-pass cell; QTF, quartz tuning fork; NNEA, normalized noise equivalent absorption.
[b]Noise measured with a lock in the integration time of 60 ms.

4.59 mV, and the standard deviation (σ) of the noise is 44.8 μV, leading to a signal-to-noise ratio of 102.5 and a 1σ detection limit of ~48.8 ppmv. Therefore, the proposed all-fiber LITES reveals a normalized noise equivalent absorption (NNEA) (1σ) of 9.66×10^{-9} cm^{-1} W · $Hz^{-1/2}$.

A detailed comparison between the free-space LITES and the all-fiber LITES was summarized in Table 1. The NNEA, which is independent of absorption line strength, optical power, and the detection bandwidth, is employed to compare the detection performance of different LITES sensors. The all-fiber LITES without free-space optics realizes a compact design due to the used HC-PCF and SMF tip. However, the HC-PCF introduces a ~10 times higher noise level due to mode interference compared to that in a free-space LITES sensor (~4 μV even with a lower lock-in integration time of 60 ms). A similar detection performance or NNEA is realized in both Ref. [9] and the proposed all-fiber LITES. Therefore, it can be inferred that the all-fiber LITES sensor will achieve ~10 times better detection performance compared with the free-space LITES sensor in Ref. [9] if the mode interference noise is suppressed effectively. The NNEAs in Refs. [4,12] are ~10 times lower than the all-fiber LITES, which mainly benefits from the high Q-factor of the QTF in a low-pressure environment and from a custom QTF. However, the same methods can be used in the all-fiber LITES for performance improvement.

As can be seen in Fig. 6(b), the mode interference noise is the dominant noise in the proposed all-fiber LITES sensor, while the dominant noise in the free-space LITES is the QTF thermal noise [12], which is usually small as can be seen from Table 1. However, when a high-power laser source is used, the thermal noise level of the QTF will inevitably increase [12], which should also be considered for the all-fiber LITES in future research. Recent research in Ref. [17] reveals that using anti-resonant fibers as a gas cell demonstrated less mode interference due to inhibited coupling between the core and the cladding modes. In addition, the anti-resonant fibers with a larger core diameter (~60 μm) compared to the HC-PCF (~10 μm) can also be used in the mid-infrared spectral region to target fundamental molecular transitions with strong absorbances. Thus, the detection performance and response time, which are related to the gas flow rate through the fiber, can be improved simultaneously.

In conclusion, we have studied an all-fiber LITES exploiting a HC-PCF and a SMF tip to overcome the limitations of size, optical alignment, and integration into photonic circuits in free-space LITES. The detection performance is limited by mode interference of a multimode HC-PCF. To further improve the detection performance of the all-fiber LITES sensor, the mode interference noise should be minimized, which can be realized by using an anti-resonant fiber instead of a HC-PCF or an additional signal processing method [15,17]. In addition, placing the QTF in a low-pressure environment for improving the Q-factor and using custom QTFs are also possible for performance improvement.

Funding. National Natural Science Foundation of China (61627823, 61775079, 61960206004); Science and Technology Development Program of Jilin Province, China (20180201046GX, 20190101016JH).

REFERENCES

1. F. Yang, W. Jin, Y. Lin, C. Wang, H. Lut, and Y. Tan, J. Lightwave Technol. **35**, 3413 (2017).
2. W. Jin, Y. Cao, F. Yang, and H. L. Ho, Nat. Commun. **6**, 7767 (2015).
3. A. A. Kosterev, Y. A. Bakhirkin, R. F. Curl, and F. K. Tittel, Opt. Lett. **27**, 1902 (2002).
4. Y. He, Y. Ma, Y. Tong, X. Yu, and F. K. Tittel, Opt. Lett. **44**, 1904 (2019).
5. L. Dong, A. A. Kosterev, D. Thomazy, and F. K. Tittel, Appl. Phys. B **100**, 627 (2010).
6. K. Liu, H. Yi, A. A. Kosterev, W. Chen, L. Dong, L. Wang, T. Tan, W. Zhang, F. K. Tittel, and X. Gao, Rev. Sci. Instrum. **81**, 103103 (2010).
7. H. Yi, W. Chen, S. Sun, K. Liu, T. Tan, and X. Gao, Opt. Express **20**, 9187 (2012).
8. L. Hu, C. Zheng, J. Zheng, Y. Wang, and F. K. Tittel, Opt. Lett. **44**, 2562 (2019).
9. Y. Ma, Y. He, Y. Tong, X. Yu, and F. K. Tittel, Opt. Express **26**, 32103 (2018).
10. J. Ding, T. He, S. Zhou, L. Zhang, and J. Li, Appl. Phys. B **124**, 78 (2018).
11. S. Zhou, N. Liu, L. Zhang, T. He, B. Yu, and J. Li, Opt. Laser Technol. **113**, 261 (2019).
12. Y. Ma, Y. He, P. Patimisco, A. Sampaolo, S. Qiao, X. Yu, F. K. Tittel, and V. Spagnolo, Appl. Phys. Lett. **116**, 011103 (2020).
13. B. Culshaw, G. Stewart, F. Dong, C. Tandy, and D. Moodie, Sens. Actuators, B **51**, 25 (1998).
14. L. Hu, C. Zheng, D. Yao, D. Yu, Z. Liu, J. Zheng, Y. Wang, and F. K. Tittel, Infrared Phys. Technol. **97**, 101 (2019).
15. F. Yang, W. Jin, Y. Cao, H. L. Ho, and Y. Wang, Opt. Express **22**, 24894 (2014).
16. S. Schilt, L. Thévenaz, and P. Robert, Appl. Opt. **42**, 6728 (2003).
17. M. Nikodem, G. Gomolka, M. Klimczak, D. Pysz, and R. Buczynski, Opt. Express **27**, 36350 (2019).